Bioresource Technology 102 (2011) 5083–5092

Contents lists available at ScienceDirect

Bioresource Technology

journal homepage: www.elsevier.com/locate/biortech

Microalgae bulk growth model with application to industrial scale systems

Jason Quinn [a,c], Lenneke de Winter [b], Thomas Bradley [a,*]

[a] Mechanical Engineering, Colorado State University, Fort Collins, CO 80521, USA
[b] Wageningen University, Bioprocess Engineering, Post Office Box 8129, 6700 EV Wageningen, Netherlands
[c] Solix Biofuels, Inc., 430 B North College Ave, Fort Collins, CO 80524, USA

ARTICLE INFO

Article history:
Received 9 November 2010
Received in revised form 5 January 2011
Accepted 6 January 2011
Available online 20 January 2011

Keywords:
Modeling
Algae
Biofuel
Photobioreactor
Life-cycle assessment

ABSTRACT

The scalability of microalgae growth systems is a primary research topic in anticipation of the commercialization of microalgae-based biofuels. To date, there is little published data on the productivity of microalgae in growth systems that are scalable to commercially viable footprints. To inform the development of more detailed assessments of industrial-scale microalgae biofuel processes, this paper presents the construction and validation of a model of microalgae biomass and lipid accumulation in an outdoor, industrial-scale photobioreactor. The model incorporates a time-resolved simulation of microalgae growth and lipid accumulation based on solar irradiation, species specific characteristics, and photobioreactor geometry. The model is validated with 9 weeks of growth data from an industrially-scaled outdoor photobioreactor. Discussion focuses on the sensitivity of the model input parameters, a comparison of predicted microalgae productivity to the literature, and an analysis of the implications of this more detailed growth model on microalgae biofuels lifecycle assessment studies.

1. Introduction

Microalgae-based biofuels have several sustainability, economic, and environmental benefits over more conventional biofuels. When compared to first-generation biofuel feedstocks, microalgae are characterized by higher solar energy yield, year-round cultivation, the use of lower quality or brackish water, and the use of less- and lower-quality land. Microalgae feedstock cultivation can be coupled with combustion power plants or other CO_2 sources to sequester GHG emissions and it has the potential to utilize nutrients from wastewater treatment facilities (Batan et al., 2010; Schenk et al., 2008; Wijffels and Barbosa, 2010). These advantages have lead to an increased interest in microalgae as a second generation feedstock for biofuels.

Analyses that have attempted to model the productivity, economics, and lifecycle environmental impacts of the latest generation of microalgae cultivation systems have relied on scale-up of laboratory data to model microalgae growth at industrial scale. Previous modeling efforts have undertaken the specific challenge of modeling growth and lipid accumulation in nutrient limited algal systems, however validation was done utilizing small-scale laboratory data (Mairet et al., 2011; Packer et al., 2010). The scaling of laboratory data has been justified due to the immaturity of the microalgae-to-biofuels process and lack of peer reviewed, published, scalable growth data. It is well-understood that these laboratory-scale processes do not accurately represent industrial-scale facilities (Chisti, 2007; Wijffels and Barbosa, 2010). To fully understand the productivity potential of microalgae-based biofuels, models must be constructed, and validated to predict the productivity of the microalgae in a realizable configuration and at industrial scale while incorporating real locational characteristics (James and Boriah, 2010).

This study presents a literature-based bulk growth model incorporating the primary factors that affect microalgae growth and lipid accumulation. This article then describes the experimental methods including the Solix research and development microalgae growth facility located at Colorado State University, and presents a direct comparison and validation of the model using actual *Nannochloropsis oculata* growth data from outdoor Solix Generation 3 photobioreactors. The discussion focuses on a sensitivity analysis and some potential applications of the model. Specifically, the model results are applied to illustrate the sensitivity of scalability calculations and life-cycle assessment (LCA) studies to the increased fidelity available from this model of microalgae growth and lipid productivity.

2. Methods

2.1. Modeling equations overview

The following sections detail the governing equations and parameters of the microalgae bulk growth and lipid production model. The purpose of the model is to accurately represent micro-

* Corresponding author. Tel.: +1 970 491 3539; fax: +1 970 491 3827.
E-mail address: thomas.bradley@colostate.edu (T. Bradley).

0960-8524/$ - see front matter © 2011 Elsevier Ltd. All rights reserved.
doi:10.1016/j.biortech.2011.01.019

algae growth and lipid accumulation of an outdoor photobioreactor. The primary factors that have been experimentally and theoretically shown to effect the productivity of microalgae are: light intensity, photosynthetic rate, respiration rate, temperature, nutrient availability, and lipid production (Richmond, 2004; Sheehan et al., 1998). The bulk model presented here takes into account all of these factors. The model incorporates 7 sub-systems defined by 16 species-specific modeling parameters. The model requires inputs of light and reactor temperature, and has outputs of biomass growth and lipid accumulation for the reactor system modeled. The origins and application of the subsystems and species parameters are detailed.

The bulk model equations and microalgae characteristics are developed from literature, coded in MatLab®, and validated with growth data of *Nannochloropsis oculata* cultivated at Solix in outdoor photobioreactors.

2.1.1. Light distribution modeling

In this model, a primary input is light which is represented as a volumetric average light intensity calculated based on light intensity at reactor surface. Mixing microalgae cultures has an effect on growth by increasing the frequency of light to dark cycling of the cells. In systems that operate at a relative low cell density, in short optical path reactors, at relatively low sparge rates, mixing dynamics will not dramatically affect the microalgae culture growth rates (Qiang and Richmond, 1996). This model therefore assumes that the culture is adapted to the average light intensity (Richmond, 2004). The alternative is to simultaneously model time-resolved microalgae growth kinetics, fluid dynamics, and light penetration, but the increase in computational cost and validation effort for this alternative is currently not justified.At low densities within the reactor, the intensity of light will fall off exponentially according to the Lambert–Beer Law (Richmond, 2004):

$$E(L) = E_0 \cdot e^{-\alpha \cdot qX_{dw} \cdot L}. \quad (1)$$

At higher densities scattering can become an important consideration for determining local light intensities (more details in Supplementary material). This model uses an average light intensity and uses Lambert–Beer for a 1st order approximation to conservatively estimate the amount of light that passes completely through the reactor, which for the reactor system modeled would only occur at low cell densities where Lambert–Beer law is applicable. The average light intensity in the plate reactor modeled can then be calculated as:

$$E_{av} = E_0 \cdot \frac{1 - e^{-\alpha \cdot qX_{dw} \cdot B}}{\alpha \cdot X_{dw} \cdot B} \quad (2)$$

2.1.2. Photosynthetic rate modeling

For this model, biomass growth is calculated based on an energy balance incorporating photosynthetic, respiration, and energy required for the uptake of nitrogen. Photosynthesis involves a series of reactions that start with light absorption, involve synthesis of NADPH and ATP as intermediate energy-conserving compounds, and lead to carbon fixation in the Calvin cycle. The carbon specific rate of this reaction (P_c) is dependent on the light intensity, light absorption, and the efficiency of using photons (see Supplementary material for more details) (Geider and Osborne, 1991; Williams et al., 2002):

$$P_c = P_{c\_calc} \cdot \left(1 - \exp\left[\frac{-\alpha \cdot \phi_m \cdot E_{av}}{P_{c\_calc}}\right]\right) \quad (3)$$

P_{c_max} is affected by two efficiency factors (see Sections 2.1.5 and 2.1.6 for definitions of φ_T and ($\phi_{qN,X_{int}}$):

$$P_{c\_calc} = P_{c\_max} \cdot \phi_T \cdot \phi_{qN,X_{int}}. \quad (4)$$

The final expression (3) balances energy flow with carbon fixation including, respiration losses, and energy loss requirements for nitrogen uptake when bioavailable nitrogen is present (more details on nitrogen effects are presented in Section 2.1.6).

2.1.3. Respiration rate modeling

This model incorporates respiration losses from metabolic costs of biosynthesis and the costs of cell maintenance. Metabolic costs such as the reduction of nitrate to ammonium and incorporation of ammonium into biomass is incorporated as a function of the specific uptake rate of nitrogen and biosynthetic efficiency which is not incorporated into the respiration portion of the model (Geider et al., 1998). Researchers in the past have shown that respiration rates during the night are the same as respiration rates during the day, indicating that maintenance respiration is neither stimulated nor inhibited by growth (Geider and Osborne, 1991). For this model maintenance respiration (rR_c) is defined as a constant.

The respiration rates observed in the field are the combination of bacterial and microalgae respiration. This model assumes that contamination levels of bacteria are insignificant; however, as described below, the respiration of the culture modeled is based on growth data that would include the effects of respiration from bacteria, if present.

2.1.4. Growth rate modeling

The model presented defines the carbon specific growth rate as a function of the photosynthetic rate, the respiration rate, and specific uptake rate of nitrogen:

$$\frac{1}{cC,X} \cdot \frac{dcC,X}{dt} = \mu = P_c - rR_c - \zeta \cdot r\mathrm{N}. \quad (5)$$

The dry weight (DW) of the biomass in the reactor (cX_{dw}) can be calculated for each time step based on the assumption that the biomass is 50% carbon. The specific growth rate, μ, is calculated at each time step and is assumed to be constant for the duration of the time step:

$$cX_{dw} = 2 \cdot cC, X_0 \cdot e^{\mu \cdot t}. \quad (6)$$

2.1.5. Temperature rate dependence modeling

In this model the temperature dependence of photosynthesis is described by the effect of temperature on ribulose-biphosphate carboxylase (Rubisco) activity. When considering a seasonal cycle, temperature is the environmental factor that consistently accounts for the largest part of the variance in growth (Geider and Osborne, 1991). This model assumes that temperature only affects the light-saturated photosynthesis rate, and not the initial slope of the photosynthesis-irradiance curve (see Supplementary material) (Geider et al., 1997). It is assumed that the reactor temperature affects the culture photosynthetic rate and respiration rate equally.

The model presented by Alexandrov and Yamagata (2007) relating thermodynamic concepts, such as activation energy, to the typical bell shape of the enzyme activity temperature curve illustrated in (7) and (8) have been adapted to this model.

$$\phi_T = \frac{2 \cdot (T)}{(1 + f^2(T))} \quad (7)$$

$$F(T) = e^{\frac{Ea}{RT_{opt}} - \frac{Ea}{RT}} \quad (8)$$

The efficiency factor for temperature (φ_T), is a dimensionless number between 0 and 1. At the optimum growth temperature $\varphi_T = 1$, and for temperatures higher or lower than the optimum temperature, $0 < \varphi_T < 1$ according to (7).

2.1.6. Nitrogen dependence modeling

For the model presented, it is assumed that microalgae growth is limited by nitrogen availability and not by phosphorus availability. The model presented incorporates nitrogen dependence modeling to accurately capture the growth and lipid production. The components of the cellular photosynthetic apparatus account for a large fraction of the total nitrogen in microalgae. Therefore, microalgae respond to a reduction in nitrogen availability by reducing the size of the photosynthetic apparatus. A linear dependence of maximum photosynthesis rates on nutrient-limited growth has been observed. Correlated with this reduction in maximum photosynthesis rate is a decrease in the proportion of cell nitrogen, which is associated with a decrease in Rubisco. In general, the light-limited photosynthesis rates are less affected by nutrient limitation than the light-saturated rates (Geider and Osborne, 1991). Geider et al. (1997) assumed in their model that nutrient-limitation affects growth rate only by imposing a limit on the light-saturated photosynthesis rate. Nutrient limitation will be modeled by multiplying maximum photosynthesis rate with an efficiency factor for nutrient-limitation ($\phi_{qN,X_{int}}$) according to the Droop model (4).The Droop model assumes that microalgal growth rate is dependent on intra-cellular nitrogen concentration (Lemesle and Mailleret, 2008):

$$\mu = \mu_{max} \cdot \left[1 - \frac{qN,X_{min}}{qN,X}\right] \tag{9}$$

The cell quota (qN,X) is defined as the mass of internal nitrogen per total mass of biomass. This quota can be experimentally measured and is time varying. The minimum cell quota (qN,X_{min}) is the internal nitrogen level where cells cease to grow. The dimensionless efficiency factor for intercellular nitrogen will therefore be described by:

$$\phi_{qN,X_{int}} = 1 - \frac{qN,X_{min}}{qN,X}. \tag{10}$$

The efficiency factor for the specific uptake rate of nitrogen considering external nitrogen concentration is treated as a Michaelis–Menten function (Geider et al., 1998; Legovic and Cruzado, 1997):

$$\phi_{qN_{ext}} = \frac{cN_{medium}}{cN_{medium} + K_N} \tag{11}$$

When the extracellular concentration of nitrogen is low or the intercellular concentration of nitrogen is high, specific uptake rate is low.

When nitrogen is present in the medium in the form of nitrate, uptake is an energy-linked process and happens mostly during daylight (Richmond, 2004). The maximum specific uptake rate of nitrogen is a function of maximum photosynthetic rate. The calculated specific uptake rate of nitrogen (rN_{calc}) is calculated by multiplying the maximum specific uptake rate of nitrogen with three efficiency factors: intracellular concentration of nitrogen efficiency (10), extracellular concentration of nitrogen efficiency (11), and temperature efficiency (7) (Geider et al., 1998):

$$rN_{calc} = rN_{max} \cdot \phi_{qN,X_{int}} \cdot \phi_{qN_{ext}} \cdot \phi_T \tag{12}$$

The specific uptake rate of nitrogen can now be defined by (13). Integration of (13) yields the total nitrogen in the biomass, (14).

$$\frac{1}{qN,X} \cdot \frac{dqN,X}{dt} = rN = \frac{rN_{calc}}{qN,X} - rR_N \tag{13}$$

$$qN,X = qN,X_0 \cdot e^{rN \cdot t} \tag{14}$$

The total remaining nitrogen in the growth media can now be calculated through mass balance.

2.1.7. Lipid accumulation modeling

The model incorporates a lipid accumulation model that has been developed to predict the lipid production of the microalgae based on a mass balance due to the effects of nitrogen. Once nitrogen is depleted, microalgae metabolism switches from protein synthesis to lipid or carbohydrate synthesis causing a change in the biomass composition (Richmond, 2004). For this model it is assumed that the microalgae metabolism is primarily protein synthesis to lipid and the protein molar percentage, the carbohydrate molar percentage, and the lipid molar percentage in the biomass stays constant:

$$\text{Biomass} = \text{Lipid} + \text{CHO} + \text{PRO} \tag{15}$$

Suen et al. (1987) reported lipid concentrations of 55% under nitrogen limited growth of *Nannochloropsis sp.* Hu and Gao (2006) found that lipid content upon nitrogen depletion increased from 9% to 62% of dry weight, while protein content decreased from 59% to 23% of dry weight in *Nannochloropsis sp.* grown under low nitrogen concentration with carbohydrate content only increased by 10% upon nitrogen depletion. These results suggest that in *Nannochloropsis sp.* metabolism almost entirely shifts from protein synthesis to lipid synthesis.

It should be noted that other environmental factors, like salinity and temperature, can also have an influence on lipid production (Richmond, 2004). Although (13) represents a 1st order relationship between lipid content and nitrogen content, validation data (presented in Section 3.3) illustrates its effectiveness.

2.2. Model parameters summary

The following section presents an overview of the inputs to the model with the specific assumptions explained. The model is based off of the cultivation of *Nannochloropsis oculata* grown in an outdoor Solix photobioreactor. Model inputs and parameters are summarized in Table 1 with ideal model outputs shown in Fig. 1.

2.2.1. Light saturation level

Researchers have shown that the light saturation of green microalgae typically occurs at 10% of full sunlight. Fabregas et al. (2004) grew *Nannochloropsis sp.* under diverse light intensities in a 12 h light, 12 h dark cycle determining a light saturation level of 220 μmol m^{-2} s^{-1}. Gentile and Blanch (2001) determined a light saturation of 180 μmol m^{-2} s^{-1} for *Nannochloropsis gaditana*. Lower values of the light saturation (74 μmol m^{-2} s^{-1}) have been reported, however those cultures where cultivated under constant light conditions (Fang et al., 2004). Considering the mixing level, density operated, diurnal light characteristics, along with the most relevant experimental data, a light saturation of 200 μmol m^{-2} s^{-1} is assumed. It is important to note that the nutrient levels can affect the light saturation value because nutrient depletion reduces the chlorophyll content of the microalgae. This effect is accounted for in this model through the efficiency factors associated with nitrogen uptake (Flynn et al., 1993).

2.2.2. Absorption coefficient

The absorption coefficient was determined experimentally for *Nannochloropsis,* 0.0752 m^2 g^{-1} (Gentile and Blanch, 2001). The absorption coefficient of microalgae will vary over the course of a batch; however the variance is not significant in this application.

2.2.3. Maximum growth rate

The maximum cell-specific growth rate represents the highest growth rate attainable in the exponential growth phase. The maximum cell-specific growth rate under nutrient rich conditions for this modeling effort is 2.5×10^{-2} h^{-1} (Flynn et al., 1993; Gentile and Blanch, 2001).

Table 1
Summary of model parameters.

Parameter	Abbreviation	Value	Unit
Light saturation level	E_k	200	μmol m^{-2} s^{-1}
Absorption coefficient	α	0.0752	m^2 g^{-1}
Maximum growth rate	μ_{max}	2.5×10^{-2}	h^{-1}
Maintenance reparation rate	rR_c	4.32×10^{-4}	h^{-1}
Biosynthetic efficiency	ζ	4	g g^{-1}
Optimum Temperature	T_{opt}	23	°C
Activation energy	E_a	63	kJ mol^{-1}
Maximum cell quota of nitrogen	qN,X_{max}	0.150	g g^{-1}
Minimum cell quota of nitrogen	qN,X_{min}	0.010	g g^{-1}
Cell quota of nitrogen of inocula	qN,X_0	0.060	g g^{-1}
Half saturation constant for nitrogen uptake	K_N	0.005	g L^{-1}
Maximum specific uptake rate of nitrogen	rN_{max}	1.5×10^{-6}	g g^{-1} h^{-1}
Maximum photosynthetic rate	P_{c_max}	3.6×10^{-2}	h^{-1}
Photon efficiency	φ_m	6.5×10^{-7}	g (μmol photons)$^{-1}$
Nitrogen respiration rate	rR_N	0	h^{-1}

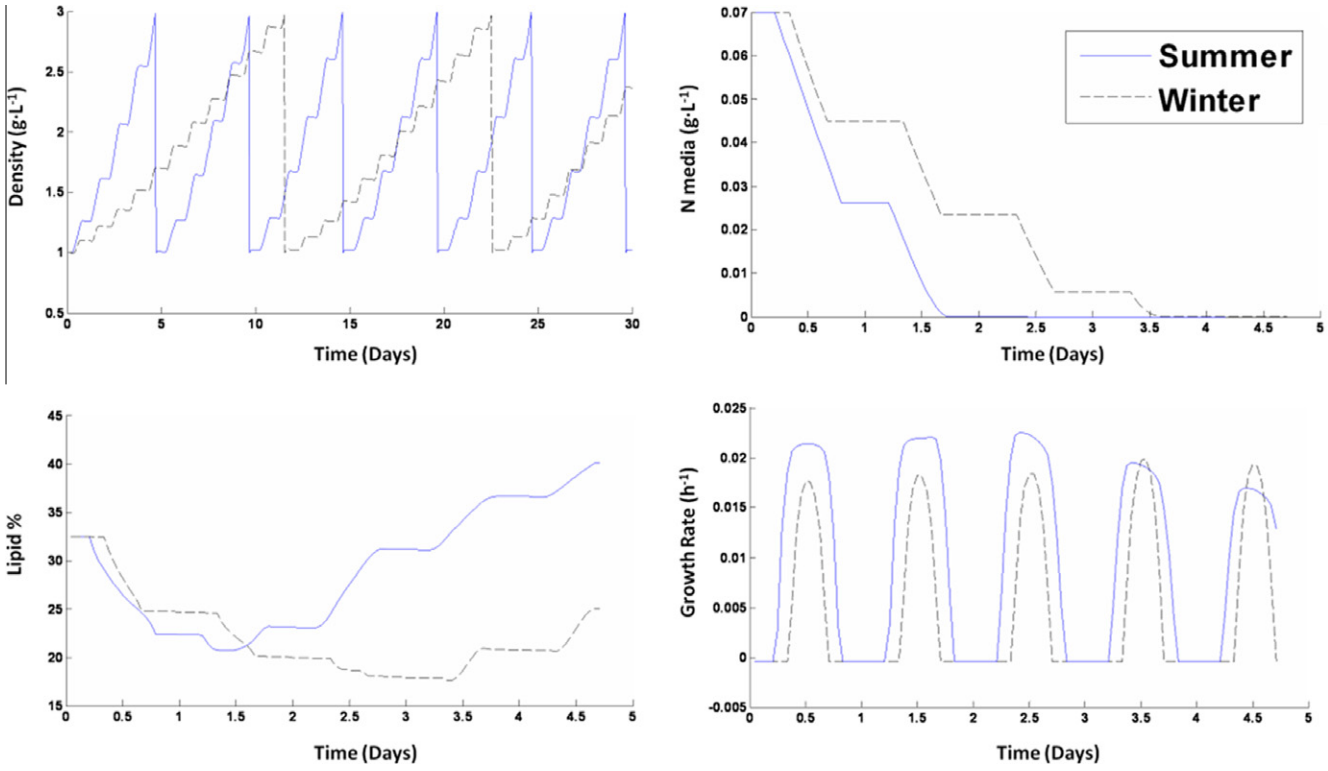

Fig. 1. Solid blue line represents results from summer-time simulation and dashed black line represents winter-time simulation. All simulations assumed ideal basin temperatures and clear sky ideal light conditions based on a geographical location of Fort Collins, Colorado using the Rest2 solar model. Top Left: Model prediction of overall culture density with harvesting at 3 g L^{-1} over a 30 day period. Top Right: Model results for bioavailable nitrogen in media over a 5 day growth period. Bottom Left: Model results for lipid accumulation over a 5 day growth period. Bottom Right: Model results for growth rate for a 5 day growth period (For interpretation of the references to color in this figure legend, the reader is referred to the web version of this article.).

2.2.4. Maintenance respiration rate

A linear relationship between the maximum photosynthetic rate and the maximum growth rate has been observed (Geider and Osborne, 1991). This observation coupled with (4) shows that the respiration rate and the maintenance respiration rate can be defined as a percentage of the maximum photosynthetic rate. For this model, a respiration rate of 2% is selected to match experimental data.

2.2.5. Biosynthetic efficiency

Energy is required for the reduction of nitrate to ammonium, incorporation of ammonium into amino acids, and polymerization of amino acids into proteins. This energy is accounted for through biosynthesis efficiency, ζ, set at 4 g biomass per g nitrogen assimilated (Geider et al., 1998). Details on the maximum and minimum nitrogen to carbon ratios are presented in Sections 2.2.8 and 2.2.9.

2.2.6. Optimum temperature

A literature review indicates the optimum temperature of *Nannochloropsis oculata* is between 21 and 24 °C (Spolaore et al., 2006). For this modeling effort an optimum temperature of 23 °C is selected.

2.2.7. Activation energy

The activation energy for this model is based on the energy required for activity of the Rubisco enzyme. Light-saturated photo-

synthesis and the carboxylase activity of Rubisco are characterized by activation energy of 54–72 kJ mol^{-1} (Geider and Osborne, 1991). A value of 63 kJ mol^{-1} has been selected for this model.

2.2.8. Maximum cell quota of nitrogen

The maximum cell quota of nitrogen is the maximum amount of nitrogen that can be contained in the cell. Analysis of the biomass produced in the Solix photobioreactor yields a maximum cell quota of 0.15 g nitrogen per g biomass and selected for this modeling effort. For comparison, Hu and Gao (2003) determined that the protein content of *Nannochloropsis sp.* ranges between 34% and 41%. This converts to a maximum cell quota of 0.07–0.09 g nitrogen per g biomass. Flynn et al. (1993) found a lower maximum cell quota of 0.2 g nitrogen per g biomass.

2.2.9. Minimum cell quota of nitrogen

Flynn et al. (1993) found a maximum carbon–nitrogen ratio of 28, corresponding to a cell quota of 0.036 g nitrogen per g biomass. Ambrose (2006) uses a smaller number, 0.0072 g nitrogen per g biomass, therefore, for this study the minimum cell quota is assumed to be between the two literature values, 0.010 g nitrogen per g biomass.

2.2.10. Cell quota of nitrogen in inocula

Inocula are obtained from a sample of a mature, harvested culture. An analysis of the biomass composition of harvested microalgae showed a protein content of 29%. Using a nitrogen-to-protein conversion factor of 4.78, the nitrogen content for inocula is set at 0.060 g nitrogen per g biomass (see Supplementary material).

2.2.11. Half saturation constant for nitrogen uptake

The half saturation constant for nitrogen uptake determines the rate at which the specific uptake rate of nitrogen declines when nitrogen concentration in the medium decreases. A value of 0.005 g L^{-1} will be assumed for this model (Ambrose, 2006).

2.2.12. Maximum specific uptake rate of nitrogen

The maximum specific uptake rate of nitrogen is a function of the maximum photosynthetic rate with units of g nitrogen per g biomass per hour:

$$rN_{max} = P_{c\_max} \cdot qN, X_{max} \tag{16}$$

From (16) the maximum specific uptake rate of nitrogen is 1.5×10^{-6} g g^{-1} h^{-1}.

2.2.13. Maximum photosynthetic rate

The maximum specific carbon photosynthetic rate is linked to the maximum growth rate and can be calculated by combining (5), (12), and (16):

$$P_{c\_max} = \frac{\mu_{max} + R_c}{1 - \zeta \cdot qN, X_{max}} \tag{17}$$

Based on these relations, P_{c_max} is calculated as 3.6×10^{-2} h^{-1}.

2.2.14. Photon efficiency

The photon efficiency in this model is a set value, because the maximum photosynthetic rate, the absorption coefficient, and the saturation parameter are set and the following identity is assumed valid:

$$E_k = \frac{P_{c\_max}}{\alpha \cdot \phi_m} \tag{18}$$

The bulk growth model, as illustrated by (18), assumes a minimum quantum requirement of approximately 46 photons, equal to a photon efficiency of 0.0217 or 6.5×10^{-7} g CH_2O (μmol photons)$^{-1}$. According to the Z-scheme of photosynthesis, E_k is 0.125 (8 mol of photons needed for production of one mole of CH_2O), representing an idealized number of photons, which is not attainable in non-idealized systems. To model realistic systems, there are other metabolic processes that must be considered, including photorespiration and losses (Geider and Osborne, 1991). These two effects significantly lower the photon efficiency below its theoretical limit. Energy required for nitrogen absorption is incorporated into the biosynthetic efficiency term not the photo efficiency term.

2.3. Experimental materials and methods

The model presented above was validated using weather and outdoor growth data from the Solix research and development facility located at Colorado State University. The following section details the cultivation system, operation, and monitoring for data collected and used in model validation.

2.3.1. Organism, culture media, and inoculation

The culture *Nannochloropsis oculata* obtained from the Provasoli-Guillard National Center for Culture of Marine Phytoplankton was cultivated in batch mode starting at 1 g L^{-1} in modified f/2–20 g L^{-1} media (0.425 g L^{-1} sodium nitrate, 0.005 g L^{-1} potassium phosphate, 1 mL L^{-1} Guillard trace metals). The microalgae was initially cultivated in flasks under 24 h low light (200 μmole m^{-2} s^{-1}) until enough mass was obtained to populate the large outdoor photobioreactors. All media are prepare and pushed through a 0.2 μm absolute filter into a tank with the required inocula where it is mixed to ensure homogeneity prior to inoculation.

2.3.2. Outdoor culture system

The reactor system modelled for this effort is based on the Solix Generation 3 photobioreactor. The thickness of an individual reactor is 0.05 m with reactors spaced at approximately 0.15 m. The growth system comprises 16 reactors constructed out of 0.12 mm polyethylene and structurally supported in a thermal basin (see Supplementary material). Mixing is provided through sparge air that is operated continuously at 2.5 L min^{-1} of sparge per liter of culture (VVM). CO_2 is supplied into the sparge air and delivered to the system with a duty cycle determined by pH feedback control (pH maintained at 7.3 ± 0.1). The reactors are operated in repeated batch mode, growing from the inoculation density of 1 g L^{-1} to a harvest density of 3 g L^{-1}. Part of the mature culture is harvested and then fresh filtered nutrient media are added such that the reactors are re-inoculated at 1 g L^{-1}.

The temperature of the culture is maintained by the thermal mass of water basin which also supplies the structural support for the reactors. The temperature was continuously monitored and maintained between 19 and 26 °C via a Marley evaporative cooling system with a capacity at the location of 270,000 BTU or Jandy Lite2 pool heater with a capacity of 325,000 BTU.

2.3.3. Growth monitoring

Two independent techniques where used for monitoring the growth of the culture. Optical density was monitored continuously using an Optech model ASD19-N absorption probe connected to a Fermenter Control Hardware A1. Datum were logged on a minute time scale and converted to dry mass using a calibration factor. The sensor was monitored for biofouling and periodically cleaned.

Manual samples of the culture were taken daily to monitor growth, nutrient content, and salinity. Samples were drawn using a 10 mL syringe through sample lines attached to sample ports at the head of the reactors. Previous sampling experimentation showed that sampling location does not affect experimental results due to the homogeneity of the culture. Manual optical density measurements at 750 nm were performed on a Hach DR5000 spec-

trophotometer (see Supplementary material for details on sample preparation).

2.3.4. Lipid assay

Lipid fractions were determined using an in situ transesterification. The following procedure was performed based on the methods of Gonzalez et al. (1998): 5 mg of microalgae sample was spun down at 4000 relative centrifugal force (RCF) for 5 min followed by the removal of the supernatant. An auto-pipette was used to dispense 2.5 mL of 0.2 N KOH in methanol onto the 5 mg microalgae pellet. Samples were pipette mixed and transferred to a glass test tube previously washed in 1% HCl acid. An additional 2.5 mL of 0.2 N KOH in methanol was added and pipette mixed. Samples were then aggressively mixed using a VWR Analog Vortex Mixer on a speed setting of 10 for 20 s followed by heating to 37 °C for 30 min. 1 mL of acetic acid and 2 mL of HPLC grade heptane were then added and the samples were aggressively mixed by using a VWR Analog Vortex Mixer on a speed setting of 10 for 20 s and then centrifuged at 2000 RCF for 5 min. The organic layer was then removed and processed in a gas chromatograph (GC) to determine lipid content and composition. GC details are presented in the Supplementary material.

3. Results and discussion

3.1. Sample growth results

The model is used to simulate microalgae growth for the ideal summer (June-solid blue line) and ideal winter (January-dashed black line) conditions based on cloud free, clear-sky solar irradiance for Fort Collins, Colorado based on the REST2 solar model, Fig. 1 (Gueymard, 2008).

There are several notable characteristics in Fig. 1. The culture is cultivated from 1 to 3 g L^{-1} for both summer-time and winter-time simulations. Nitrogen uptake is a direct function of light, thus in the winter the uptake of the bioavailable nitrogen from the media takes significantly longer. The overall growth in the winter is significantly lower than summer due to lower light intensity and shorter days. The specific growth rate during the dark period is negative due to respiration effects for both cases. The results presented in Fig. 1 are typical of the function of growth observed at the Solix research and development facility.

3.2. Growth model validation

Validation of the bulk growth model was performed by quantitatively and qualitatively comparing modeled results with real world growth results. Validation of the model is based on the American Institute of Aeronautics and Astronautics definition of model validation with the intended use of the model presented is accurately capture the bulk growth and lipid production of an outdoor scalable photobioreactor system (AIAA, 1998).

Two panels (A & B) were monitored during peak summer-time (high-light data); panel A for approximately 3 weeks followed by panel B for an additional three. Winter-time (low-light data) was also collected for approximately 3 weeks in November and December to complete the data set. Reactor configuration, light, and temperature data (see Supplementary material) from the location of the outdoor photobioreactor installation was used as primary inputs to the model with 1 week of summer-time (high-light data) and 1 week of winter-time (low-light data) model productivity results plotted against real time growth data and manual OD 750 samples, Fig. 2.

As shown in Fig. 2, the model qualitatively captures the growth trends from day to day including respiration during the dark period. A more quantitative comparison of the modeled growth versus actual growth on a minute time scale is presented in Fig. 3 for summer-time (high-light data) and winter-time (low-light data).

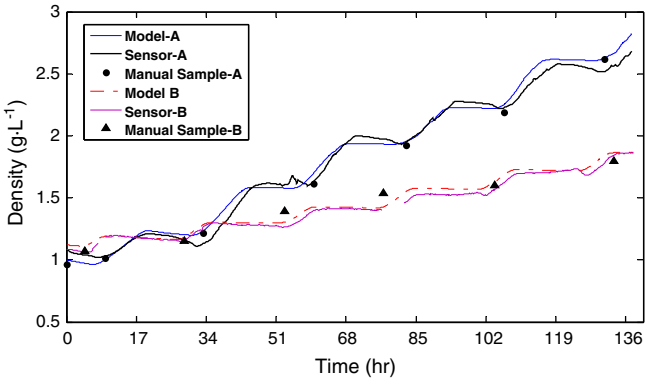

Fig. 2. Plot of model output (Model), institute OD sensor (Senor), and manual samples performed daily (Manual Sample) for two reactors A and B are presented. Approximately one week of high light (June 13–18) for reactor A and approximately one week of low light (November 11–16) for reactor B raw growth data from the sensor and manual OD and model simulated growth are presented.

The maximum deviations over the 9 weeks worth of data presented in predicted biomass versus measured biomass are 0.26 and −0.23 g L^{-1} respectively. Analysis of the difference between

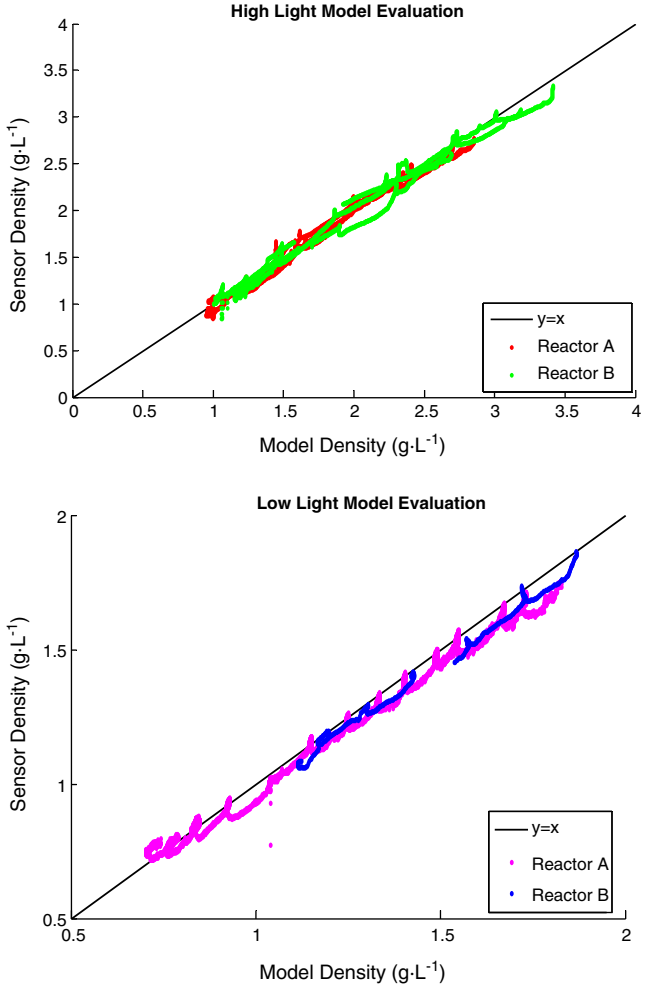

Fig. 3. Plot of predicted versus actual daily change in density on a minute time scale for 6 weeks of growth during high light conditions, summer (top) and 3 weeks of growth during low light conditions, winter (bottom).

the measured biomass density and the predicted biomass density on a minute time scale shows a mean of $-0.00339\ g\ L^{-1}$ with a standard deviation of $0.0678\ g\ L^{-1}$ ($n = 70{,}224$), indicating the model accurately captures the bulk growth of the system however, slightly overestimates the growth. The model is shown to be robust up to 160 h under real diurnal light of varying intensity with a maximum overestimation of $0.15\ g\ L^{-1}$ (9.2%) and under estimation of $0.06\ g\ L^{-1}$ (−2.8%) and average over prediction of 3% for the 8 batches modeled, Table 2.

The validated biomass model incorporates real diurnal light and meteorological effects to accurately capturing the bulk biomass growth of the scalable outdoor photobioreactor system modeled. For the purposes of predicting bulk biomass growth under instantaneous and batch operation for real-world climactic and thermal conditions, the model is considered validated to within the accuracies described above.

3.3. Lipid model validation

Lipid accumulation in microalgae can be triggered by a variety of variables including but not limited to nutrients, pH, salinity, temperature, and light (Fabregas et al., 2004; Fang et al., 2004; Hu and Gao, 2006; Richmond, 2004; Suen et al., 1987). The system being modeled here enters a nutrient depleted stress mode. Lipid levels as predicted by the model to reach a maximum of 44%. Lipid percentages in literature for *Nannochloropsis oculata* grown in batch mode have been reported to vary with a maximum of 55% (Suen et al., 1987). Lipid percentage of the biomass was monitored on a regular basis for 3 weeks of operation and is presented along with lipid percentage as predicted by the model in Fig. 4.

The model accurately captures the trend of the lipid content. The reactors modeled did achieve a maximum lipid percentage of 51%, 9 days after inoculation during normal operation, which is slightly higher than the model. Biologically, cultures grown in batch mode will transition from linear growth into stationary growth depending on nutrient availability and other factors. A different physiological model representing growth and lipid accumulation for the stationary phase is required to accurately represent growth and composition of the microalgae. In stationary growth, energy dedicated to lipid accumulation would need to be considered in more detail.

For the purposes of predicting biomass lipid content under batch operation for real-world climactic and thermal conditions, the model is considered validated with a standard deviation of error of 8.8% lipid by mass.

Table 2
Summary of total change in biomass as predicted by the model and measured by the sensor for 8 batches, (6 high light and 2 low light) including total time of the batch.

Reactor	Model ($\Delta g\ L^{-1}$)	Actual ($\Delta g\ L^{-1}$)	Batch Length (h)
A-high light	1.89	1.82	135
A-high light	1.77	1.62	157
A-high light	1.56	1.54	167
A-low light	1.08	0.99	199
B-high light	2.08	2.14	147
B-high light	2.27	2.20	168
B-high light	1.68	1.60	166
B-low light	0.74	0.78	301

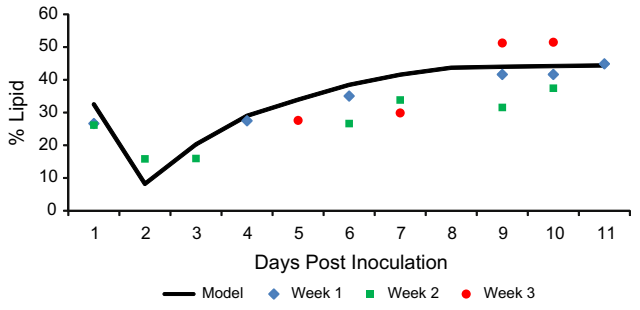

Fig. 4. Plot of lipid percentage in biomass for 3 weeks of continual monitoring over 11 day period overlaid on top of predicted lipid percentage from model.

3.4. Sensitivity analysis

A sensitivity analysis was performed on all inputs to the model. The sensitivity analysis involved increasing and decreasing each input parameter by 20% and evaluating the biomass production at 100 h (see Supplementary material). An analysis of variance was used to estimate *t*-ratios for each input parameter. Results are presented in Fig. 5.

As illustrated in Fig. 5, variables associated with growth parameters, light modeling, and nitrogen factors have the largest effect on the biomass productivity. The model is insensitive to variations in some parameters such as molecular weight of the microalgae.

Results from this sensitivity analysis are important to consider when adapting the model to other microalgae species. Factors with a *t*-ratio greater than the *t*-ratio at the 95% confidence interval have a large effect on the models output thus need to be known to higher degree of certainty than characteristics inside this interval.

3.5. Implications of improved modeling on practical production potential of microalgae

The majority of studies that contemplate the large scale land use requirements of biodiesel from microalgae are calculated by linearly scaling small-scale laboratory productivity data. This simplistic scaling leads to erroneous assumptions about industrial growth facility function, and a large uncertainty in the modeled productivity potential of microalgae. Values reported in literature range from $12\ m^3\ ha^{-1}\ yr^{-1}$ reported by Schenk et al. (2008) to $184.0\ m^3\ ha^{-1}\ yr^{-1}$ reported by Yeang (2008) with Huntley and Redalje (2007), Sheehan et al. (1998), Wijffels and Barbosa (2010), Hirano et al. (1998), Campbell et al. (2010), Lardon et al. (2009), and Chisti (2007, 2008) reporting values between these extremes.

The validated model presented in this study provides a more detailed representation of industrial scale microalgae growth facilities to more accurately represent the true current microalgae growth potential. To understand the effects that this more detailed model will have on these scalability assessments, the model will be used to simulate a year of growth for a proposed high productivity location.

The southwestern US is primarily where deployment of first generation, large-scale microalgae facilities has been proposed. Historical weather data from Yuma, Arizona were input to the model because Yuma has the most cloud free days in the US (242 days) with 90% of annual sunlight hours being cloud free. This location assumption assumes that water and CO_2 are readily available and that optimum thermal conditions exist in the thermal basin. Two different harvesting schemes were simulated: "time harvest", where harvest of the culture occurs at 160 h or $3\ g\ L^{-1}$ (whichever occurs first), which is more representative of the function of the research and development facility used in model validation, and "density harvest", where culture is harvested at $3\ g\ L^{-1}$ regardless of elapsed time.

These results represent current maximum yields which might be achievable in the continental US due to the ideal thermal conditions and ideal geographic location selected. The time harvest simulation results in productivity of $5.72 \times 10^4\ kg\ ha^{-1}\ yr^{-1}$ of

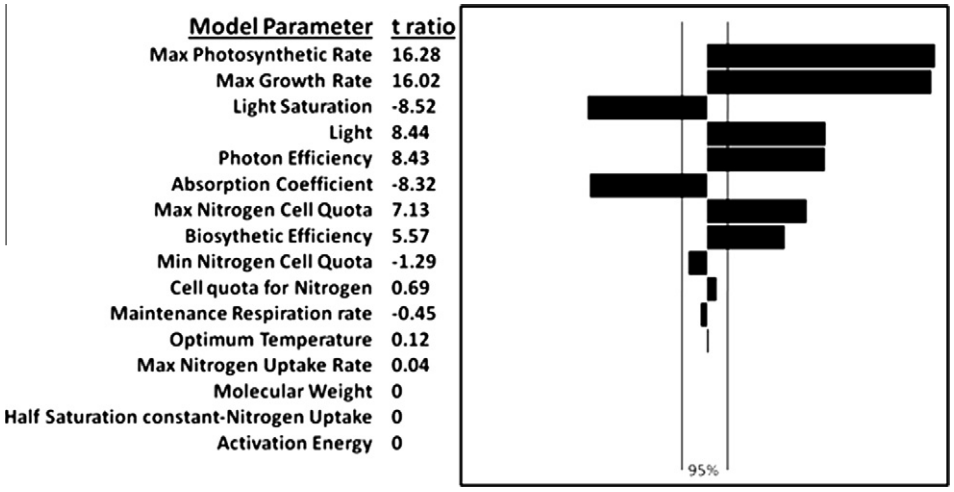

Fig. 5. Sensitivity of model inputs presented in tornado plot format. Model inputs were altered by ±20% with total predicted biomass production after 100 h compared to baseline scenario. Vertical lines represent 95% confidence interval.

biomass or 26.452 $m^3\ ha^{-1}\ yr^{-1}$ of oil. For the density harvest, the simulation results in a productivity of 5.79×10^4 kg $ha^{-1}\ yr^{-1}$ of biomass or 28.744 $m^3\ ha^{-1}\ yr^{-1}$ of oil. The time harvest scheme represents a −1.1% difference in biomass but a −8.7% difference in oil production, relative to the density harvest scheme. Culture growth in the high-light, long days of summer facilitates the growth of the culture to 3 g L^{-1} in a short period of time. In the winter, the lower light intensities and shorter days mean 3 g L^{-1} is not achievable in a 160 h time period, thus the microalgae is harvested before reaching maximal lipid content.

The validated model predicts a realistic annual productivity potential that is 7 times lower than the highest value reported in the literature surveyed, and is significantly lower than the median productivity reported in literature, as shown in Table 3. The reduced productivity can be attributed to a variety of effects that are present in this model but are not present in other models. The development of the more detailed bulk growth and lipid productivity model allows for the consideration of the effects of facility scale, harvesting strategies, meteorological effects, seasonal effects, and more. Although the resulting productivity of 26.5 $m^3\ ha^{-1}\ yr^{-1}$ of oil may still represent an optimistic estimation of the annual production of oil at a large-scale photobioreactor facility, this result represents the most realistic industrial scale productivity value to date.

Table 3
Table comparing reported productivity potentials (some calculations performed for comparison purposes) from various sources. Some authors reported a range of productivity potential, consequently the high (††) and low (†) values are repeated.

Source	Oil ($m^3\ ha^{-1}\ yr^{-1}$)	Notes
Schenk et al. (2008)†	12	30%[a]
Chisti (2008)†	20.7	20%[a], ρ_{oil} = 880 kg m^{-3}
Bulk model, this study	26.5	Idealized, Time Harvest, Yuma, AZ
Huntley and Redalje (2007)†	30.7	40%[a], ρ_{oil} = 880 kg m^{-3}
Wijffels and Barbosa (2010)	40	50%[a], 3% solar conversion efficiency
Yeang (2008)†	46	
Hirano et al. (1998)	49.8	40%[a], ρ_{oil} = 880 kg m^{-3}
Lardon et al. (2009)	51.4	50%[a], ρ_{oil} = 880 kg m^{-3}
Chisti (2008)b††	51.8	50%[a], ρ_{oil} = 880 kg m^{-3}
Batan et al. (2010)†	51.8	50%[a], ρ_{oil} = 880 kg m^{-3}
Chisti, 2007†	58.7	30%[a]
Sheehan et al. (1998)†	62.2	50%[a], ρ_{oil} = 880 kg m^{-3}
Campbell et al. (2010)	62.3	50%[a], ρ_{oil} = 880 kg m^{-3}
Schenk et al. (2008)††	98.5	50%[a]
Huntley and Redalje, 2007††	99.5	40%[a], ρ_{oil} = 880 kg m^{-3}
Batan et al. (2010)††	103.8	50%[a], ρ_{oil} = 880 kg m^{-3}
Sheehan et al. (1998)††	124.4	50%[a], ρ_{oil} = 880 kg m^{-3}
Chisti (2007)††	136.9	30%[a]
Yeang (2008)††	184	

[a] Oil content in biomass.

3.6. Life cycle assessment (LCA) modeling

LCA is a fundamental tool that has been used to evaluate the sustainability of biofuels. The results from LCA are highly sensitive to engineering model assumptions, definitions of system boundaries, life-cycle inventories, process efficiencies, and functional units. Increasing interest in microalgae as a secondary feedstock for transportation fuels has lead to multiple LCA studies. Inherent in these studies is an engineering model of the microalgae to biofuels process that incorporates a growth model.

The majority of the microalgae LCA published to date use a simplistic growth model based on a daily productivity number obtained from a small scale laboratory growth facility. Large scale productivity over an entire year is then calculated based on this laboratory number. Batan et al. (2010), Lardon et al. (2009), Hirano et al. (1998), and Campbell et al. (2010) all use a fixed growth rate between 10 and 30 g $m^{-2}\ d^{-1}$ (3.6×10^4–11.0×10^4 kg $ha^{-1}\ yr^{-1}$) in their growth models. Due to the lack of published data on realistic, large-scale productivities, three of the studies discussed above run multiple scenarios using a range of fixed growth rates in modeling the productivity of large-scale facilities (Batan et al., 2010; Campbell et al., 2010; Lardon et al., 2009). This is indicative of the sensitivity of LCA analysis to the growth models implemented in the process model.

This study presents a validated, large-scale growth model that accurately captures diurnal and annual weather impacts on microalgae growth. The model can be integrated with historical weather data and can be used to more accurately represent the growth of microalgae at specific geographical locations. The majority of the geographic locations of the LCA studies surveyed are warm coastal regions. Meteorological data for the costal location of San Diego, California were used to illustrate realistic biomass productivity and compare results to the LCA studies discussed. The thermal basin temperature was assumed to be regulated for optimum growth and the time harvest strategy was used, resulting in a productivity of 5.42×10^4 kg $ha^{-1}\ yr^{-1}$ of biomass or 15 g $m^{-2}\ d^{-1}$. This analysis

shows that the current realizable productivity of microalgae is less than the median of the typical growth rates used in the LCA models surveyed.

To enable more accurate environmental assessments of biofuel from microalgae, LCA studies need to use more accurate growth models. To date, LCA studies have made geographic location assumptions based on material availability and nearness to markets, but have not included the effect of geographic location on growth. The model developed for this study will enable a more accurate representation of feasible large-scale production, thus improving the environmental assessment of the microalgae to biofuels process.

4. Conclusion

A literature-based bulk growth and lipid production model was constructed incorporating 16 species-specific variables, using light and temperature as primary inputs. Validation of this model was done utilizing 9 weeks of stochastic weather and growth data from a large scalable outdoor photobioreactor cultivating *Nannochloropsis oculata*. Historical weather data for the idealized solar location of Yuma, Arizona was used to illustrate the current productivity potential of 5.72×10^4 kg ha^{-1} yr^{-1} of biomass or 26.4 m^3 ha^{-1} yr^{-1} of oil given optimum thermal conditions. The model was also used to illustrate the requirement for more in-depth and accurate growth modeling for LCA analysis.

Acknowledgements

We gratefully acknowledge financial support provided by Solix Biofuels, Inc and data collection and processing support from Chris Tuner, Mark Machacek, Pete Hentges, Kristina Weyer, John Walden, and Zach Turner.

Appendix A. Nomenclature

Symbol	Description	Unit
B	reactor thickness	m
Biomass	biomass composition	–
CHO	percent carbohydrate in biomass	–
Lipid	percent lipid in biomass	–
cN_{medium}	nitrogen concentration in media	g·L^{-1}
PRO	percent protein in biomass	–
cX_{dw}	biomass concentration in reactor	g·L^{-1}
E (L)	light intensity at distance L	μmol·m^{-2}·s^{-1}
E_0	light intensity incident on reactor wall	μmol·m^{-2}·s^{-1}
Ea	activation energy carboxylation Rubisco	J·mol^{-1}
E_{av}	average light intensity in photobioreactor	μmol·m^{-2}·s^{-1}
E_k	light saturation level	μmol·m^{-2}·s^{-1}
f(T)	temperature function	–
K_N	half saturation constant for nitrogen uptake	g·L^{-1}
L	distance from reactor wall into culture	m
P_c	photosynthetic rate (carbon)	h^{-1}
P_{c_calc}	calculated maximum photosynthetic rate (carbon)	h^{-1}
P_{c_max}	maximum photosynthetic rate (carbon)	h^{-1}
cC,X	carbon content of biomass in reactor	g·L^{-1}
cC,X_0	carbon content of biomass at previous time step in reactor	g·L^{-1}
qN,X	cell quota of nitrogen in biomass	g ·g $^{-1}$
qN,X_0	amount of nitrogen present at previous time step in biomass	g·g^{-1}
qN,X_{max}	maximum cell quota for nitrogen in biomass	g·g $^{-1}$
qN,X_{min}	minimum amount of nitrogen in biomass	g·g^{-1}
R	universal gas constant	J·K^{-1}·mol^{-1}
rR_c	maintenance respiration rate (carbon)	h^{-1}
rR_N	respiration constant for nitrogen	h^{-1}
rN	specific uptake rate of nitrogen	h^{-1}
rN_{calc}	calculated specific uptake rate of nitrogen	g·g $^{-1}$·h^{-1}
rN_{max}	maximum specific uptake rate of nitrogen	g·g $^{-1}$h^{-1}
t	time	seconds
T	bath temperature	°C
T_{opt}	optimum growth temperature	°C
α	absorption coefficient	m^2·g^{-1}
ζ	biosynthetic efficiency	g·g $^{-1}$
μ	carbon specific growth rate	h^{-1}
$μ_{max}$	Maximum carbon specific growth rate	h^{-1}
$φ_m$	photon efficiency	g·(μmol photons)$^{-1}$
$φ_{qN\ ext}$	uptake of external nitrogen concentration efficiency	–
$φ_{qN,X\ int}$	uptake of internal nitrogen concentration efficiency	–
$φ_T$	temperature efficiency factor	–

Appendix B. Supplementary data

Supplementary data associated with this article can be found, in the online version, at doi:10.1016/j.biortech.2011.01.019.

References

AIAA, 1998. Guide for the verification and validation of computational fluid dynamics simulations. Reston, VA.
Alexandrov, G.A., Yamagata, Y., 2007. A peaked function for modeling temperature dependence of plant productivity. Ecol. Model. 200, 189–192.
Ambrose, R.B., 2006. Wasp7 benthic algae-model theory and users guide. USEPA, office of research and development. Athens, Georgia.
Batan, L., Quinn, J., Willson, B., Bradley, T., 2010. Net energy and greenhouse gas emission evaluation of biodiesel derived from microalgae. Environ. Sci. Technol. 44, 7975–7980.
Campbell, P.K., Beer, T., Batten, D., 2010. Life cycle assessment of biodiesel production from microalgae in ponds. Bioresour. Technol. 102, 50–56.
Chisti, Y., 2007. Biodiesel from microalgae. Biotechnol. Adv. 25, 294–306.
Chisti, Y., 2008. Biodiesel from microalgae beats bioethanol. Trends Biotechnol. 26, 126–131.
Fabregas, J., Maseda, A., Dominguez, A., Otero, A., 2004. The cell composition of *Nannochloropsis sp* changes under different irradiances in semicontinuous culture. World J. Microbiol. Biotechnol. 20, 31–35.
Fang, X., Wei, C., Cai, Z.L., Fan, O., 2004. Effects of organic carbon sources on cell growth and eicosapentaenoic acid content of *Nannochloropsis sp*. J. Appl. Phycol. 16, 499–503.
Flynn, K.J., Davidson, K., Leftley, J.W., 1993. Carbon–nitrogen relations during batch growth of *Nannochloropsis oculata* (*eustigmatophyceae*) under alternating light and dark. J. Appl. Phycol. 5, 465–475.
Geider, R.J., Osborne, B.A., 1991. Algal photosynthesis: the measurement of gas exchange and related processes. Chapman and Hall, New York. 256 pp.

Geider, R.J., MacIntyre, H.L., Kana, T.M., 1997. Dynamic model of phytoplankton growth and acclimation: responses of the balanced growth rate and the chlorophyll a: carbon ratio to light, nutrient-limitation and temperature. Mar. Ecol.-Prog. Ser. 148, 187–200.

Geider, R.J., MacIntyre, H.L., Kana, T.M., 1998. A dynamic regulatory model of phytoplanktonic acclimation to light, nutrients, and temperature. Limnol. Oceanogr. 43, 679–694.

Gentile, M.P., Blanch, H.W., 2001. Physiology and xanthophyll cycle activity of *Nannochloropsis gaditana*. Biotechnol. Bioeng. 75, 1–12.

Gonzalez, M.J.I., Medina, A.R., Grima, E.M., Gimenez, A.G., Carstens, M., Cerdan, L.E., 1998. Optimization of fatty acid extraction from *Phaeodactylum tricornutum* UTEX 640 biomass. J. Am. Oil Chem. Soc. 75, 1735–1740.

Gueymard, C.A., 2008. Rest2: high-performance solar radiation model for cloudless-sky irradiance, illuminance, and photosynthetically active radiation – validation with a benchmark dataset. Solar Energy 82, 272–285.

Hirano, A., Hon-Nami, K., Kunito, S., Hada, M., Ogushi, Y., 1998. Temperature effect on continuous gasification of microalgal biomass: theoretical yield of methanol production and its energy balance. Catal. Today 45, 399–404.

Hu, H.H., Gao, K.S., 2003. Optimization of growth and fatty acid composition of a unicellular marine picoplankton, *Nannochloropsis sp.*, with enriched carbon sources. Biotechnol. Lett. 25, 421–425.

Hu, H.H., Gao, K.S., 2006. Response of growth and fatty acid compositions of *Nannochloropsis sp* to environmental factors under elevated CO_2 concentration. Biotechnol. Lett. 28, 987–992.

Huntley, M.E., Redalje, D.G., 2007. CO_2 mitigation and renewable oil from photosynthetic microbes: a new appraisal. Mitig. Adapt. Strat. Glob. Change. 12, 573–608.

James, S.C., Boriah, V., 2010. Modeling algae growth in an open-channel raceway. J. Comput. Biol. 17, 895–906.

Lardon, L., Helias, A., Sialve, B., Stayer, J.P., Bernard, O., 2009. Life-cycle assessment of biodiesel production from microalgae. Environ. Sci. Technol. 43, 6475–6481.

Legovic, T., Cruzado, A., 1997. A model of phytoplankton growth on multiple nutrients based on the Michaelis–Menten-Monod uptake, Droop's growth and Liebig's law. Ecol. Model. 99, 19–31.

Lemesle, V., Mailleret, L., 2008. A mechanistic investigation of the algae growth "Droop" model. Acta Biotheor. 56, 87–102.

Mairet, F., Bernard, O., Masci, P., Lacour, T., Sciandra, A., 2011. Modelling neutral lipid production by the microalga *Isochrysis aff, galbana* under nitrogen limitation. Bioresour. Technol. 102, 142–149.

Packer, A., Li, Y., Andersen, T., Hu, Q., Kuang, Y., Sommerfeld, M., 2010. Growth and neutral lipid synthesis in green microalgae: a mathematical model. Bioresour. Technol. 102, 111–117.

Qiang, H., Richmond, A., 1996. Productivity and photosynthetic efficiency of *Spirulina platensis* as affected by light intensity, algal density and rate of mixing in a flat plate photobioreactor. J. Appl. Phycol. 8, 139–145.

Richmond, A., 2004. Handbook of microalgal culture biotechnology and applied phycology. Oxford, UK.

Schenk, P.M., Thomas-Hall, S.R., Stephens, E., Marx, U.C., Mussgnug, J.H., Posten, C., Kruse, O., Hankamer, B., 2008. Second generation biofuels: high-efficiency microalgae for biodiesel production. BioEnergy Res. 1, 20–43.

Sheehan, J., Dunahay, T., Benemann, J., Roessler, P., 1998. A look back at the US department of energy's aquatic species program: Biodiesel from algae. NREL/TP-580-24190. Available from: <www.nrel.gov/docs/legosti/fy98/24190.pdf>.

Spolaore, P., Joannis-Cassan, C., Duran, E., Isambert, A., 2006. Optimization of *Nannochloropsis oculata* growth using the response surface method. J. Chem. Technol. Biotechnol. 81, 1049–1056.

Suen, Y., Hubbard, J.S., Holzer, G., Tornabene, T.G., 1987. Total lipid production of the green-alga *Nannochloropsis sp* QII under different nitrogen regimes. J. Phycol. 23, 289–296.

Wijffels, R.H., Barbosa, M.J., 2010. An outlook on microalgal biofuels. Science 329, 796–799.

Williams, P.J., Thomas, D.N., Reynolds, C.S., 2002. Phytoplankton productivity: carbon assimilation in marine and freshwater ecosystems. Oxford, UK.

Yeang, K., 2008. Biofuel from algae. Arch. Des. 78, 118–119.